International Journal of Minerals, Metallurgy and Materials
Volume 28, Number 1, January 2021, Page 1
https://doi.org/10.1007/s12613-020-2119-8

Invited Review

Application and prospective of 3D printing in rock mechanics: A review

Yong-tao Gao[1,2], *Tian-hua Wu*[1,2], *and Yu Zhou*[1,2]

1) Key Laboratory of Ministry for Efficient Mining and Safety of Metal Mines, University of Science and Technology Beijing, Beijing 100083, China
2) School of Civil and Resource Engineering, University of Science and Technology Beijing, Beijing 100083, China
(Received: 27 March 2020; revised: 22 May 2020; accepted: 16 June 2020)

Abstract: This review aims to discuss the application and development of three-dimensional printing (3DP) technology in the field of rock mechanics and the mechanical behaviors of 3D-printed specimens on the basis of various available printing materials. This review begins with a brief description of the concepts and principles associated with 3DP, and then systematically elaborates the five major applications of 3DP technology in the field of rock mechanics, namely, the preparation of rock (including pre-flawed rock) specimens, preparation of joints, preparation of geophysical models, reconstruction of complex rock structures, and performance of bridging experimental testing and numerical simulation. Meanwhile, the mechanical performance of 3D-printed specimens created using six different printing materials, such as polymers, resin, gypsum, sand, ceramics, and rock-like geological materials, is reviewed in detail. Subsequently, some improvements that can make these 3D-printed specimens close to natural rocks and some limitations of 3DP technology in the application of rock mechanics are discussed. Some prospects that are required to be investigated in the future are also proposed. Finally, a brief summary is presented. This review suggests that 3DP technology, especially when integrated with other advanced technologies, such as computed tomography scanning and 3D scanning, has great potential in rock mechanics field.

Keywords: three-dimensional printing (3DP); rock mechanics; 3DP material; rock analogue; 3DP geotechnical model; numerical simulation

1. Introduction

Rock mechanics, related to the research on rock response (rock mass) to an imposed disturbance aroused by natural (e.g., tectonic movement) or engineering procedures (e.g., excavation), is a discipline that combines geology and mechanics. Rock mechanics is also a basic subject in many engineering disciplines (e.g., mining, civil, hydraulic, petroleum, underground, and geological engineering). Therefore, investigating rock mechanics is of great significance in studying and predicting the mechanical behaviors of engineering rock masses in these fields [1–2].

The geological environment determines the complex physical and mechanical characteristics of rock, such as nonlinearity, discontinuity, heterogeneity, and anisotropy, all of which lead to an increase in the difficulty of using traditional theoretical research methods to study the response of rock under stress. Experimental (e.g., *in-situ* [3] and laboratory [4–6] (most commonly used)) and numerical testing [7–8] have become important research means, with which rock properties are explored. However, rock specimens with the same properties can neither be manufactured nor tested twice, causing the results and findings to possibly be unrepresentative of the intrinsic variability in rocks.

Three-dimensional printing (3DP) technology is recently explored and applied to rock mechanics field; to an extent, this approach addresses issues such as the preparation of identical specimens or visualization of the inside of intact rocks, thereby opening new opportunities in the study of rock mechanics [9–12].

3DP technology was first proposed in the United States in the 1980s and is known as rapid prototyping technology which has been developed for over 30 years. Hull [13] first introduced the stereo lithography apparatus (SLA) method in 1986 and received a patent grant which is a milestone in 3DP technology development [14]. In the same year, he established the first 3DP device in the world, and the 3D Systems Corporation manufactured the world's first 3D printer, the SLA-250. Since then, 3DP technology has developed rapidly. Recently, various 3DP technologies exist, such as fused deposition modeling (FDM), 3DP, SLA, and selective laser sintering (SLS), whose differences are manifested in two aspects: prototyping technology and printing material [15–18]. Different 3DP technologies have their own unique prototyp-

Corresponding author: Yu Zhou E-mail: westboy85@ustb.edu.cn

ing principles and corresponding suitable printing materials. However, these technologies have two common features, that is, layer-by-layer superimposed prototyping of materials under the control of computers [19] and general printing procedures consisting of four stages. Take 3DP technologies for preparing rock specimens as an example to illustrate the four stages: i) establish a 3DP target rock model designed by AutoCAD [15,20–21] or extracted by computed tomography (CT) scanning (Fig. 1), and then convert the 3D rock model into an STL format file that may be recognizable by most 3D printers; ii) perform slice processing, and then set appropriate print parameters (layer thickness, fill ratio, and output path) for the 3D printer; iii) print a target rock solid model layer-by-layer on the basis of the defined operating rules; iv) treat the printed physical rock models via postprocessing, such as polishing until smooth. Fig. 1 presents the general procedures for preparing specimens by using 3DP technologies coupled with CT scanning technology.

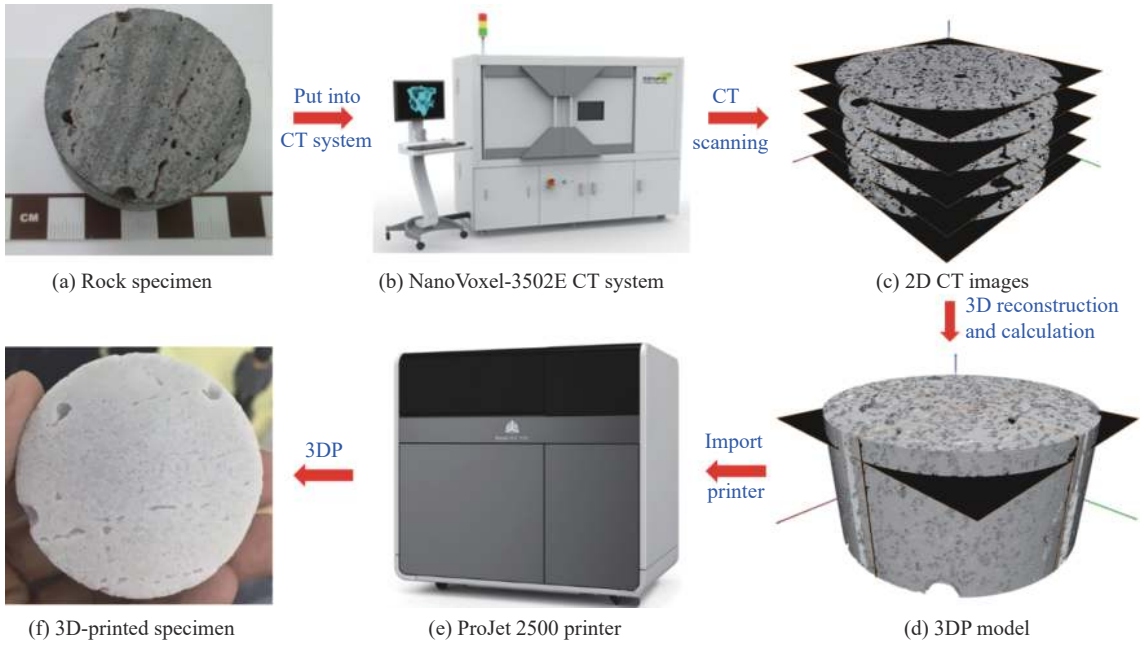

Fig. 1. General procedures for preparing specimens using 3D-printed technologies coupled with CT scanning technology.

Only few comprehensive reviews discussed the application of 3DP technology in the field of rock mechanics. Gell *et al.* [22] simply reviewed three 3DP materials, namely, polylactic acid (PLA), a gypsum-like material, and sand, which were used to prepare 3D-printed rock specimens, and compared the mechanical properties of 3D-printed and natural rock specimens to verify the validity of 3DP materials; this work was covered in the present review. Bishwal [23] presented only a general review of the potential advantages of 3DP in rock mechanics. The review on the application of 3DP technology in the field of rock mechanics is neither complete nor systematic. Consequently, a comprehensive review is essential for research to offer a deep understanding of and further explore the application of 3DP technology in the field of rock mechanics.

In this review, five major applications of 3DP in rock mechanics are systematically elaborated in detail. All studies available to authors (110 references in total) regarding this topic are extensively reviewed. Our review has four sections. Section 1 provides a brief introduction of the development of 3DP technology. Section 2 systematically reviews the details of the five aspects of 3DP application in rock mechanics, namely, i) the preparation of rock (or pre-flawed rock) specimens, ii) preparation of natural or artificial joints, iii) reconstruction of complex rock structures, iv) preparation of a geotechnical physical model, and v) creation of a virtual bridge connecting rock mechanics experiments and numerical simulations. Moreover, in the first aspect of the application, a thorough comparison of the mechanical performance of the 3D-printed specimens of different materials and those of natural rocks is presented. Section 3 comprehensively discusses several improvements that can make a 3D-printed model further similar to natural rock with respect to mechanical behaviors. Certain current limitations and future prospects of 3DP technology in the application of rock mechanics are also discussed from three main aspects. Finally, Section 4 provides a brief summary for each application.

2. Research situation of 3DP in rock mechanics

With the explosive development and widespread application of 3DP technology, a technical innovation to the field of rock mechanics and geotechnical engineering is possible. Although such an application in this field is limited, such an ap-

plication has become a reality; this development is summarized in detail via the following five specific topics.

2.1. Specimen preparation in rock mechanics experiments

2.1.1. Comparison of mechanical performance between 3D-printed and natural rocks

Various available 3DP materials have currently been applied in rock specimen fabrication [12,24–29]. Fig. 2 [30] and Table 1 show several commonly used and available 3D-printed-based rock specimen preparation methods and related materials.

When 3DP technology is used in the preparation of experimental rock specimens, conducting and comparing them with natural rock specimens is important to explore the potential feasibility and validity of using 3D-printed rock in place of natural rock. The reason is that rock specimens based on different 3D-printed materials and methods can show significant differences in their mechanical performance.

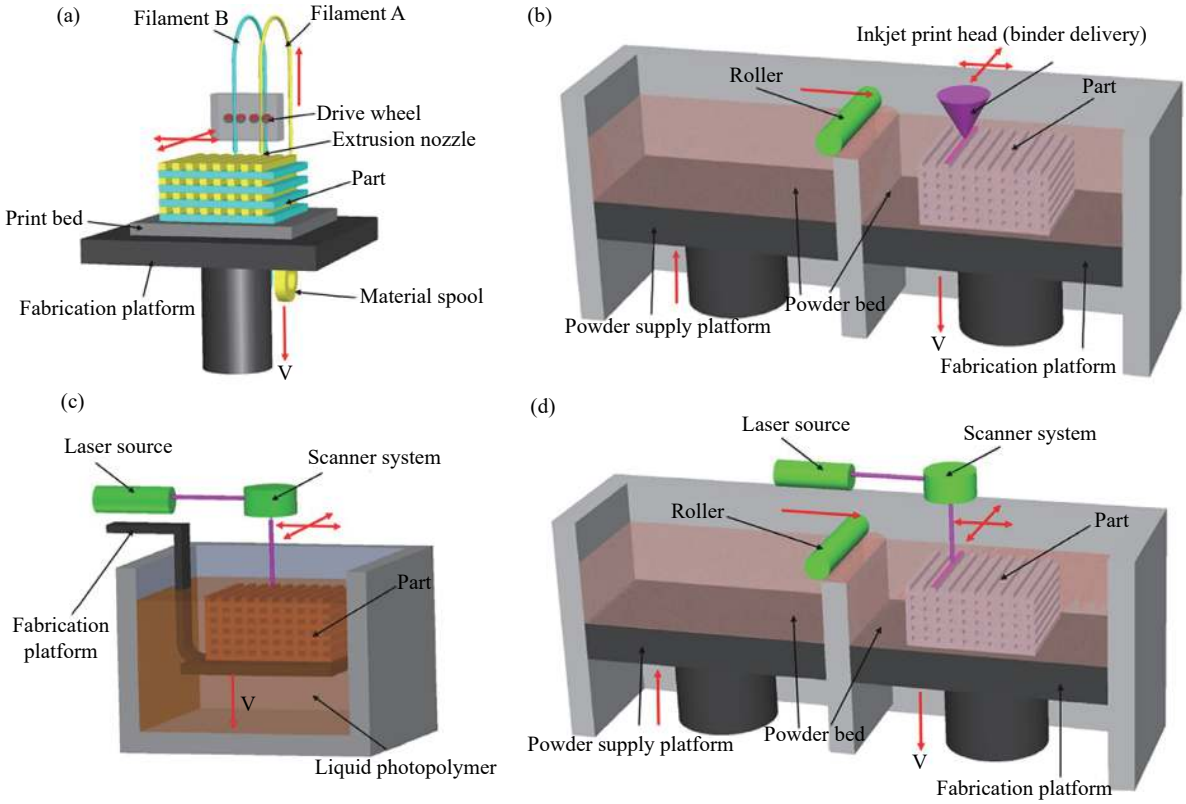

Fig. 2. Schematics for the prototyping principle of various 3DP technologies: (a) FDM technology; (b) 3DP technology; (c) SLA technology; (d) SLS technology. Reprinted from *Composites Part B*, 110, X. Wang, M. Jiang, Z.W. Zhou, J.H. Gou, and D. Hui, 3D printing of polymer matrix composites: A review and prospective, 442, Copyright 2017, with permission from Elsevier.

Table 1. Several available rock specimen preparation methods and corresponding materials

Specimen preparation method	Schematic for the method	Printing materials	Available 3D printer
FDM	Fig. 2(a)	PLA	FDM printer [15]
SLA	Fig. 2(c)	Vero-Clear; resin	Object Connex 500 [17]
3DP	Fig. 2(b)	Gypsum; sand; ceramics	ZPrinter 450 [16]
SLS	Fig. 2(d)	Sand	Sinter Station 2500 [18]
Chemical reaction	—	Geological materials	Geological Material 3D printer [12]

In 2015, Jiang and Zhao [10] conducted a few uniaxial compression tests on 3D-printed PLA specimens and discovered that PLA is a highly ideal elastoplastic material, but its failure exhibits a ductility characteristic. Song *et al.* [15] and Jiang *et al.* [24] also observed the same phenomenon in PLA rock that was significantly different from that in common natural rock, suggesting that PLA seems to be more analogous to metal materials than rocks. Interestingly, another investigation proposed that the mechanical characteristics of Vero-Clear (a transparent polymer) printed rock are extremely similar to those of natural coal [9], attributing to the fact that the overall properties, such as uniaxial compression

strength (UCS), elastic modulus, and Poisson's ratio, of 3D-printed rock are comparable with those of the prototype coal specimen. Unfortunately, a considerable discrepancy was found in the tensile and compression strengths between these two materials. Moreover, Vero-Clear displays the same ductile behavior as PLA in continuous uniaxial loading [31–32]. All these results imply that 3DP with polymer exhibits the inability of this material to sufficiently reproduce the mechanical behaviors of brittle natural rocks with high strength. Improving the brittleness of polymer materials may be one of the most important topics in the study of the mechanical performance of natural rocks using this material.

In one study [27], transparent resin material was considered to be the most appropriate material for simulating hard brittle rock because compared with the mechanical properties of several other materials, those of transparent resin material, such as brittleness, strength, and tension–compression strength ratio, are more similar to real rock. In this respect, a research team [26,33–34] continued to implement a series of quasi-static and dynamic tests on 3D-printed resin and natural rock specimens. They found that the static mechanical properties of the 3D-printed resin specimen, including UCS, failure mode, brittleness behavior, and uniaxial stress–strain curve, are remarkably similar to those of the natural volcanic rock. The difference, however, is that the peak strain of the 3D-printed specimen is greater than that of the volcanic rock, implying that the former has a higher elastic modulus than the latter (Fig. 3 [33]). Moreover, the dynamic test results demonstrated that to an extent, similarities exist in the failure mode and dynamic cracking evolution of 3D-printed and natural rock specimens. Their further research again suggested that resin material has great potential and prospects in the replication of the mechanical behaviors of hard brittle rock. In addition, its transparency is quite beneficial for studying the fracture evolution mechanism of rock.

In recent years, gypsum powder has been used in rock specimen preparation to investigate its potential in replicating mechanical rock properties [16,35]. Song *et al.* [15] believed that a 3D-printed gypsum specimen resembles real rock in terms of its deformation and failure characteristics, such as a mixed failure pattern; the specimen also showed a certain ductility (Figs. 4(a) and 4(b)). However, compared with the PLA specimen [10], although the gypsum specimen has a higher brittle characteristic and is closer to the failure mode of natural shale [36], it exhibits a lower compressive strength (less than 10 MPa) [20], as illustrated in Figs. 4(c)–4(e). Therefore, the high strength of the gypsum material should be further investigated for its improvement; in this way, real rock can be simulated well. Simultaneously, Song *et al.* [15] also investigated the tensile properties of gypsum specimens, demonstrating that the splitting failure mode and corresponding load history of the gypsum specimens show good similarity to those of the natural rock specimens, except the granite specimens. These results suggest that the brittleness and strength of the printed material require improvement, and its stiffness should be maintained in future studies.

The possibility of applying sand powder in the fabrication of 3D-printed sandstone analogues has been studied [24,37–38]. A few comparisons of the mechanical features of 3D-printed and natural sandstones were made [39–40]. The UCS, tensile behavior, fracture roughness, and crack evolution of 3D-printed sandstone specimens exhibit a similarity to those of weak and high-porosity real sandstone specimens, particularly for the sandstone analogue that consists of quartz sand with furan binders, revealing that the sandstone analogue also shows a low strength characteristic; hence, some further improvements must be made to simulate natural sand-

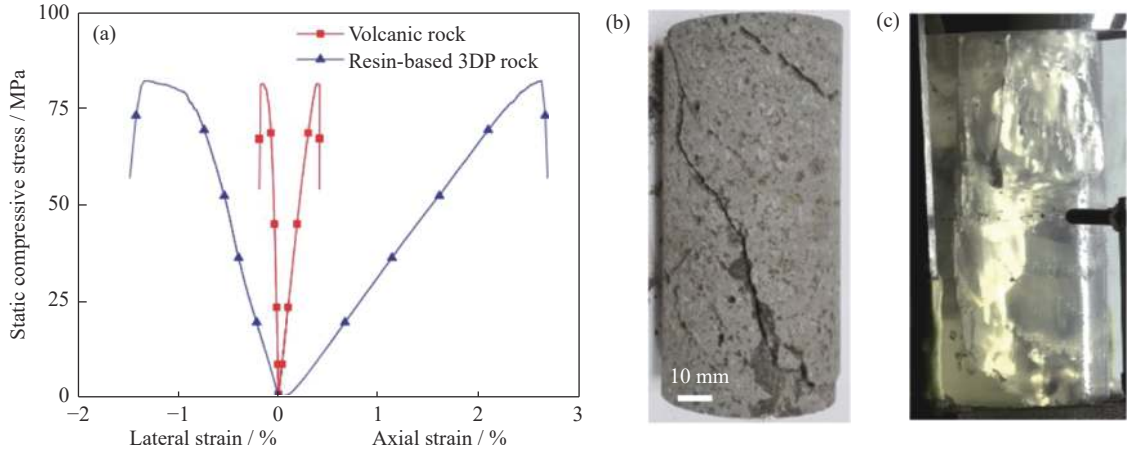

Fig. 3. Comparison of the (a) stress–strain curves and (b, c) failure modes of resin-based 3D-printed and natural volcanic rocks in static uniaxial compression tests. Reprinted from *Int. J. Rock Mech. Min. Sci.*, 106, J.B. Zhu, T. Zhou, Z.Y. Liao, L. Sun, X.B. Li, and R. Chen, Replication of internal defects and investigation of mechanical and fracture behaviour of rock using 3D printing and 3D numerical methods in combination with X-ray computerized tomography, 198, Copyright 2018, with permission from Elsevier.

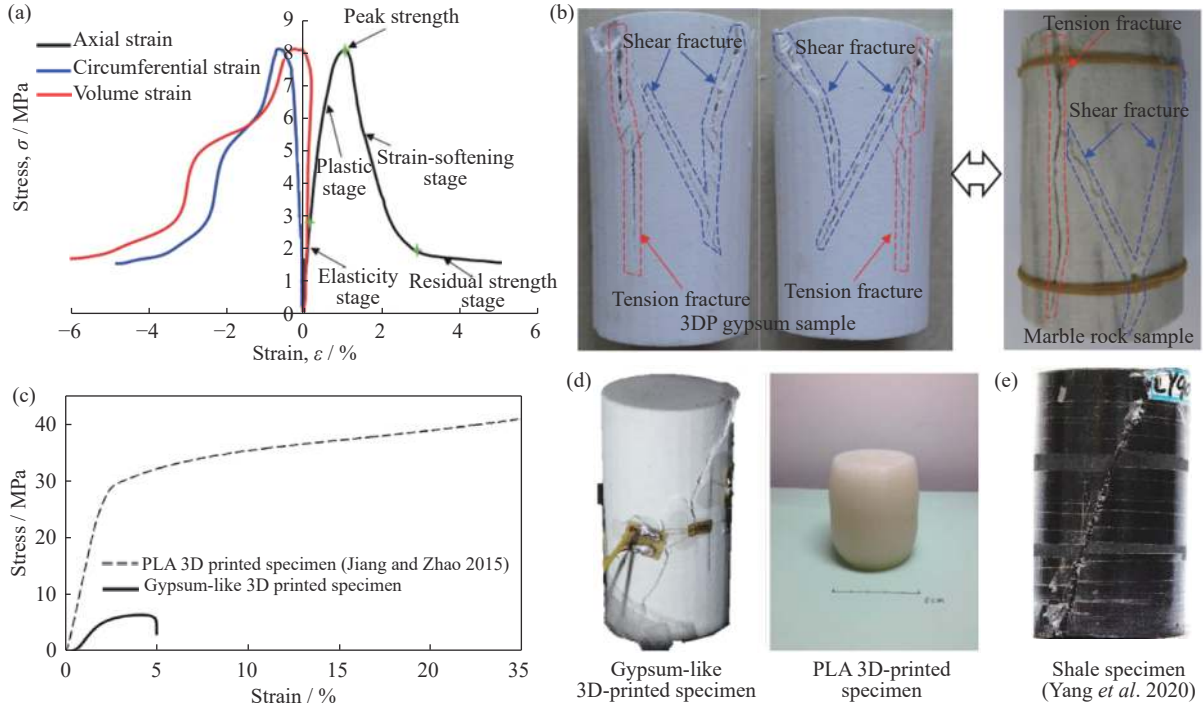

Fig. 4. Experimental results from uniaxial compression test: (a) stress–strain behavior and (b) failure mode of 3D-printed gypsum rock; comparison of the (c) stress–strain behaviors and (d) failure modes of gypsum and PLA specimens; (e) failure mode of Shale specimen. (a) and (b) are reprinted by permission from Springer Nature: *Rock Mech. Rock Eng.*, Feasibility investigation of 3D printing technology for geotechnical physical models: Study of tunnels, L.B. Song, Q. Jiang, Y.E. Shi, X.T. Feng, Y.H. Li, F.S. Su, and C. Liu, Copyright 2018; (c) and (d) are reprinted by permission from Springer Nature: *Rock Mech. Rock Eng.*, Investigation of dynamic crack coalescence using a gypsum-like 3D printing material, C. Jiang, G.F. Zhao, J.B. Zhu, Y.X. Zhao, and L.M. Shen, Copyright 2016; (e) is reprinted by permission from Springer Nature: *Rock Mech. Rock Eng.*, Experimental study on mechanical behavior and brittleness characteristics of Longmaxi formation shale in Changning, Sichuan basin, China, S.Q. Yang, P.F. Yin, and P.G. Ranjith, Copyright 2020.

stone with different strengths and stiffness. Similar to the gypsum or resin-based rock mentioned above, the vertical strain of these specimens is significantly higher than that of natural sandstone when failure occurs, which may be due to the high porosity of the 3D-printed sandstone. Moreover, a similar result (3D-printed sandstone with a larger volumetric strain than that of natural rock) can also be observed under triaxial stress situations [41], indicating that the 3D-printed sandstone displays a greater compressibility than real sandstone. However, a trend exists in which the peak deviator stress (σ_1–σ_3) increases as the confining stress (σ_3) increases in the 3D-printed sandstone, which is analogous to natural sandstone. Interestingly, the failure mode and stress–strain behavior of the 3D-printed sandstone from the uniaxial testing in the study of Tian and Han [42–43] were similar to those of natural sandstone (some deformation curves almost coincided). Fortunately, the result showed that the peak strain of the 3D-printed sandstone is nearly equal to that of natural sandstone, indicating that they have similar mesostructures, such as porosity, which may be dominated by 3DP technology. Their research outcomes describe the fact that 3D-printed rock possesses a great potential to simulate and replicate the mechanical properties of natural rock.

At present, almost no detailed and well-informed studies on the mechanical performance of ceramic-based 3D-printed rock are available [27]. Existing research asserts that 3D-printed ceramic specimens are unsuitable for simulating natural brittle rock due to their insufficient strength (less than 3 MPa) and brittleness. Although firing is traditionally able to increase the strength and brittleness of ceramics, the results of these studies indicate that 3D-printed ceramic rock affected by temperature variation is prone to generate unexpected cracks that cause swelling and crushing during the firing procedure. This reason may explain why such a material is currently used infrequently in rock mechanics studies. Inspired by the resin material, attempting to adopt a low-temperature treatment of ceramic specimens in further studies may achieve satisfactory results.

In 2019, Feng *et al.* [12] proposed an innovative 3DP technology of a rock-like geological material consisting of cementing materials (e.g., cement and gypsum) and aggregates (e.g., silica sand) in view of the fluid properties of geological materials. Subsequently, they performed a uniaxial compression test on a 3D-printed rock-like geological mater-

ial specimen. The results demonstrated that the 525R Portland-cement-based 3D-printed specimen can be employed to replicate certain classes of layered rock with respect to the stress–strain curve and failure mode. Moreover, the printed specimen showed favorable brittleness and moderate strength in the absence of other processing techniques. This research suggested that rock-like geological materials may be more advantageous in natural rock simulation than the several materials mentioned above.

2.1.2. Preparation of a rock-like specimen with pre-existing flaws

Recently, 3DP technology has been introduced in the preparation of rock-like material specimens, and it has provided new opportunities for creating pre-existing flaws with various controllable geometries in rock-like material specimens, resulting in an approach that is more favorable than conventional methods (e.g., high-pressure water-jet cutting [44] and handcrafting [45–46]) because it allows accurate fabrication, various geometries, and high repeatability [47].

To date, the published literature on printing materials applied in the preparation of flawed specimens focuses on the following four types, namely, transparent resin, gypsum, sand powder, and polymer [24,42,48–50]. Due to the high transparency and photoelasticity of the resin material, it displayed certain superiorities that directly enabled us to monitor and analyze the fracture mechanism in real time. With the help of photoelastic technology, the stress field evolution process inside 3DP pre-flawed specimens subjected to compressive loads was also characterized and visualized during crack propagation over other opaque materials, such as gypsum [33,51–52]. An investigation on the volumetric fracturing properties of 3D-printed resin rock specimens with one or two pre-existing 3D flaws under uniaxially compressive loads was recently performed [21]. A few clear differences were found in the crack evolution mechanism between printed resin rock with 3D flaws and those with two-dimensional (2D) flaws, that is, wing cracks that initiated from the 3D flaw tips had a limited range of propagation, and these secondary cracks were the cause of the failure of the 3D-printed flawed specimen. Conversely, in the 2D situation, the wing cracks initiated at the 2D flaw tips and propagated through the specimen to the boundaries, causing the appearance of failure.

In the study of Jiang *et al.* [20], a sequence of continuous photographs showed the initiation, propagation, and coalescence of cracks in the 3D-printed gypsum flawed specimen during dynamic split Hopkinson pressure bar (SHPB) tests which were recorded by high speed photography. A comparison was subsequently made among the photographs of 3D-printed flawed specimens and cemented specimens and a corresponding numerical model of a higher order displacement discontinuity method (HDDM) [53–54], suggesting a good similarity among these results, that is, not all wing cracks and cracks can coalesce at the tips of pre-existing fissures; they may initiate at the tips, and then coalesce in the middle of pre-existing fissures (Fig. 5). However, the fracture behaviors in the cemented specimens and numerical model were the results of a static compressive load. Therefore, whether the crack evolution of the 3D-printed flawed gypsum specimen under static loading is similar to that under dynamic loading still requires further research.

Similarly, Sharafisafa *et al.* [11], in 2018, conducted a few quasi-static Brazilian disk tests on a 3D-printed flawed gypsum specimen, and a digital image correlation (DIC) method was used to capture the crack evolution process. Their research indicated that the mechanical characteristics and fracture behaviors of this 3DP material agree to an extent with those of real brittle flawed rocks; 3DP integrated with DIC technology also exhibited applicability and capability in flexible specimen preparation, such as pre-existing flaw implementation, via the real time and accurate capture of the crack evolution. Another study [55], published in the following year, revealed that the pre-existing flaw filling has a great impact on the mechanical properties and crack evolution of this 3D-printed flawed specimen, that is, the specimen with filling displayed high peak strength and experienced a large fracture area.

2.2. Preparation of natural or artificial joints

The joints across a rock mass play an extremely significant role in the mechanical properties of the rock mass [56]. Currently, mainstream approaches, including *in-situ* (virgin joints), experimental (artificial joints), and numerical direct shear tests, allow us to exhaustively investigate the shear mechanical properties of natural joints in rock masses [57–58]. However, the preparation of jointed specimens in a direct shear test has always been a challenging problem (e.g., the vulnerability, poor consistency, and non-repeatability of virgin rock joints in *in-situ* tests [59] and idealized artificial joints with respect to a regular surface morphology for experimental tests [60]). In a new method [61–62], silicone rubber or separation film is used to duplicate the virgin rock joint surface to form a parent joint surface mold; a parent mold is then used to cast a batch of joint specimens to address certain related problems, although this approach still results in a lack of precision. Fortunately, by learning from this approach, the novel technology of 3DP has been successfully applied in the preparation and design of joint molds with a natural or an artificial joint surface morphology because of its high precision and flexibility [24,63–66].

One representative application for 3DP in this respect is to manufacture a 3D-printed mold with a typical Barton's joint profile [67]. In view of this 3D-printed mold, a physical joint specimen reflecting a Barton's profile was subsequently produced by casting using a similar material, such as gypsum plaster [68–72]. Moreover, a concrete joint specimen was

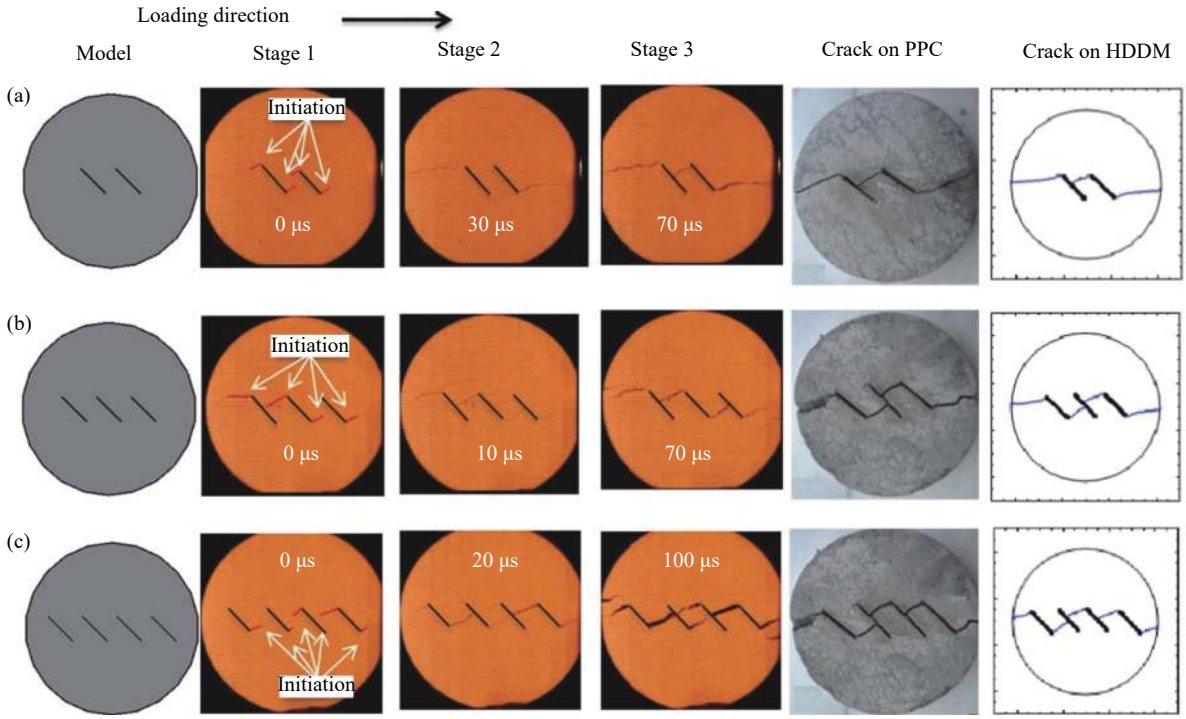

Fig. 5. Comparison of the coalescence evolution of three various 3D-printed specimens (in orange), cemented specimen, and HDDM numerical model with multiple pre-existing fissures (PPC—Portland pozzolana cement). The images of model, stage 1, stage 2, stage 3, and crack on PPC are reprinted by permission from Springer Nature: *Rock Mech. Rock Eng.*, Investigation of dynamic crack coalescence using a gypsum-like 3D printing material, C. Jiang, G.F. Zhao, J.B. Zhu, Y.X. Zhao, and L.M. Shen, Copyright 2016; The images of crack on HDDM are reprinted by permission from Springer Nature: *Arabian J. Geosci.*, Experimental and numerical analysis of Brazilian discs with multiple parallel cracks, H. Haeri, A. Khaloo, and M.F. Marji, Copyright 2015.

cast on the basis of a 3D-printed PLA mold with a Barton's profile in the research of Jiang *et al.* [24]. They declared that a 3D-printed PLA mold can replicate a Barton's joint profile with great precision and efficiency. This conclusion considers two aspects: i) a morphological comparison of the joint specimens' roughness and primary Barton's profile demonstrates good consistency; ii) the shearing deformation curves of these joint specimens, under identical testing situations, are also highly consistent (Fig. 6). Notably, the shearing deformation curves in Fig. 6(c) exhibit a plastic deformation with a certain rheological property, that is, a continuous change in the curve slopes and no obvious stress peak or stress drop are observed in the curves which are analogous to those of soft joints [73].

Another important application is that with the assistance of 3D scanning technology, 3DP allows us to reconstruct the morphology of natural joints [24,74–75], which may be a good solution to the problems faced by *in-situ* shear testing. The general processes described in the work of Jiang *et al.* [24,76] mainly include three procedures: i) 3D scanning technology enables us to obtain the point cloud data of the morphology of virgin rock joints, and such data can be used to reconstruct a model of virtual natural rock joint surface; ii) tangible molds with the morphology of natural joints may be produced using 3DP; iii) synthetic specimens with natural joints are created through manual casting on the basis of a previous 3D-printed mold. To verify the accuracy of these approaches, a geometrical comparison among the 2D profiles of natural joints, 3D-printed joint molds, and casted concrete joints was performed. The results suggested that the three profile lines in the same position matched well, and that maximum geometrical error did not exceed 2.4%. In addition, the results of direct shear testing on the two types of concrete joint specimens with different joint roughness coefficients (JRCs) indicated that their shearing deformation curves were basically the same, and that the maximum shear strength error did not surpass 6.7%, exhibiting a higher accuracy than that of conventional replicated rock joints (8%–20%) [77–78]. The study showed that 3DP allows us to produce joint specimens with favorable precision and uniform mechanical properties, which can further promote the investigation of the mechanical behaviors of virgin rock joints.

In this application, 3DP technology is only used to manufacture joint molds with high accuracy, whereas the actual testing specimen is artificially cast from similar materials. This process of casting may cause a testing specimen to exhibit a relatively high degree of heterogeneity. Consequently, similar to the present work of Li *et al.* [79], further research should determine how to create testing joint specimens dir-

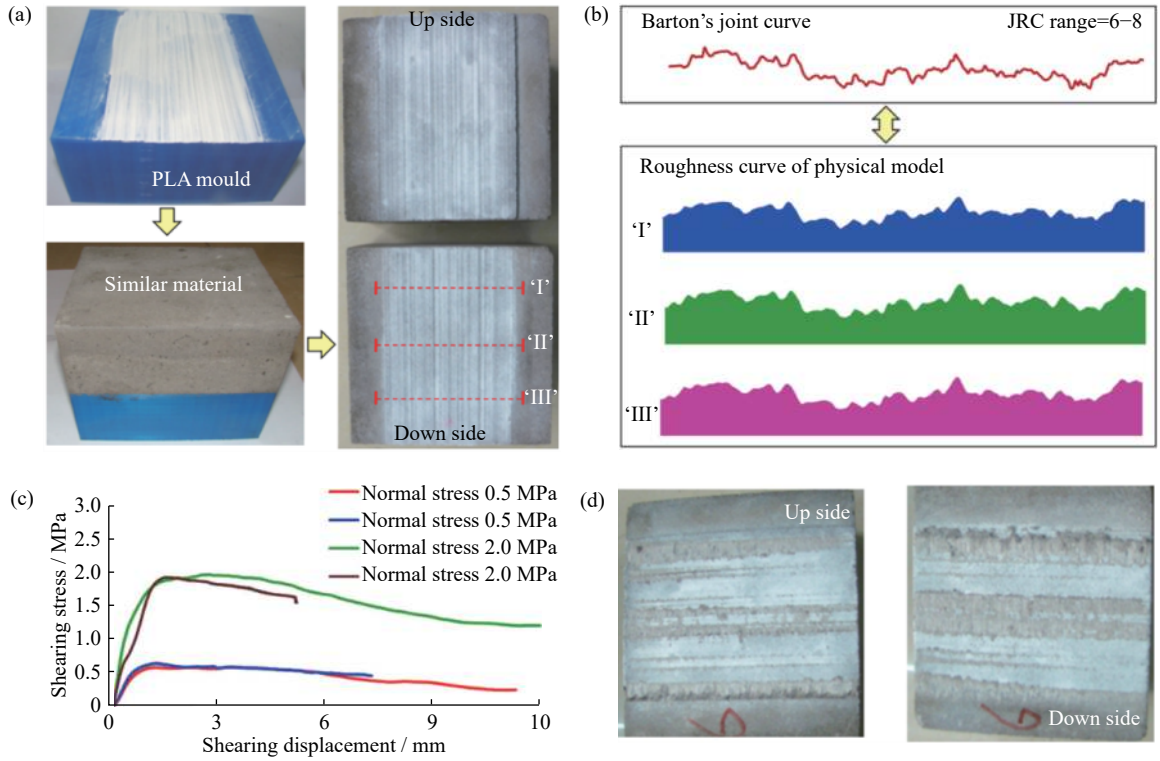

Fig. 6. Plots showing the (a) 3D-printed mold and concrete joint specimen, (b) comparison of joint specimens' roughness and primary Barton's profile (JRC—Joint roughness coefficient), (c) shearing deformation curves, and (d) sheared surface. Reprinted by permission from Springer Nature: *Acta Mech. Sin.*, Modeling rock specimens through 3D printing: Tentative experiments and prospects, Q. Jiang, X.T. Feng, L.B. Song, Y.H. Gong, H. Zheng, and J. Cui, Copyright 2016.

ectly via 3DP using similar materials which may acquire additional satisfactory and accurate results.

2.3. Reconstruction and visualization of complex internal rock structure

Reservoir rock includes complex internal structures that consist of pore and fracture networks and occupy a fairly central role in the exploitation of unconventional resources in terms of petroleum, natural gas, shale gas, and coalbed methane because their characteristics (e.g., connectivity, pore throat distribution, pore size, and coordination number) are inextricably connected to the storage energy and seepage behavior of reservoirs [80–81]. Accordingly, the accurate characterization and visualization of the internal structure of reservoir rock are the keys to investigating and analyzing the petrophysical properties of reservoirs, especially their permeability, and to addressing various practical engineering problems [9].

3DP can convert a virtual complex digital model obtained from CAD design, tomography, or microscopy into a tangible physical body at different scales, thus providing a novel opportunity for replicating and reproducing the interior complex and disordered structure of rock that may be investigated experimentally [24,33,82–84]. The pore network structure [85], fracture network structure [9], and aggregate structure [32] in rock to date have been reconstructed and characterized via 3DP coupled with X-ray CT, enabling us to establish a precise digital structure model of prototype rock.

A series of similar studies by Ishutov and his team [85–91] showed that the 3D pore network structure (proxy) of various reservoir sandstones from CT information (e.g., Berea, Idaho Gray, and Fontainebleau sandstones) was reproduced through various 3DP materials (gypsum, plastic, and resin). However, due to the limitations of the resolution of the 3D printer, a reproduction at the original scale of the sandstone failed, and the specimens had to be rescaled to the digital model dimension to create a magnified 3D-printed pore model. Their next primary research focus was a comparison of the petrophysical properties (e.g., porosity, permeability, and pore throat size) of the 3D-printed pore network model, digital model, and natural rock via mercury porosimetry, CT, helium porosimetry, etc., indicating discrepancies in certain petrophysical properties, such as porosity. A similar finding was also mentioned in the study of Kong *et al.* [92]. Multiple factors determined these discrepancies, such as 3D printer resolution, postprocessing (e.g., cleaning methods), validation means, and even 3DP methods. 3D printer resolution may be one of the most critical reasons for this result. Encouragingly, although discrepancies are exhibited, 3D-printed pore network models may be repeatedly used in various

experimental tests (e.g., fluid-flow and core-flood experiments) which offer new ways to quantitatively assess and analyze the characteristics and processes of reservoir rock (e.g., fluid transport properties [93]). In a similar way, a pore network of carbonate rock at its original scale was replicated by Head and Vanorio [94] who focused on an investigation of various pore network structures that influence transport properties at multiple scales. However, they did not discuss the model accuracy. With the assistance of photoelasticity, Ju *et al.* [95–96] not only accurately reconstructed and visualized the local 3D-printed pore structure of Berea sandstone using a transparent photopolymer material but also quantitatively described the stress evolution of intricate pore structures subjected to successive loads, indicating that the integration of 3DP with other advanced technologies is more likely to become a mainstream tool to further investigate the properties of complex rock masses.

For the fracture network structure reconstruction inside a rock, Ju *et al.* [9] first reproduced a potential coal-like rock photopolymer specimen that contains a complex internal fracture structure identical to a natural coal rock by using 3DP in accordance with its CT scanning data. Significantly, to reflect and embody the heterogeneity of the coal-like specimen, they adopted an approach in which a matrix and a fracture network are created using two different photopolymer materials to assign their corresponding attributes. This study also illustrated that the fracture network characteristics of the 3D-printed coal-like rock specimen are identical to those of the natural coal rock. However, a discrepancy was found in their mechanical properties, such as compressive strength, suggesting that the mechanical similarities between the reconstructed model and natural rock still need to be enhanced.

Other investigations on the reconstruction of aggregate structures inside rocks (e.g., glutenite rock and even rock-like concrete material) were recently conducted [17,25,32]. Likewise, as previously mentioned, the matrix and gravel are respectively characterized by transparent (Vero-Clear) and opaque (RGD 525) printing materials by using multiple-nozzle 3D printer which can visually reproduce heterogeneous aggregated models. Although 3DP enables us to visualize and accurately reconstruct complex structures in rocks, coupled with photoelastic and stress freezing technologies, and can reproduce and characterize the evolution of the stress fields surrounding complex structures, such as pores, fractures, and aggregate network structures, the mechanical properties of the 3D-printed models with complex structures identical to those of natural rock or rock-like materials (e.g., coal, sandstone, glutenite, and even concrete) appear to diverge from their prototype. Consequently, improvements in the mechanical properties of the reconstructed models for a good simulation of natural rocks remain necessary. If certain improvements, such as novel 3DP materials or posttreatment methods, can make the mechanical properties similar to those of natural rocks, then a tremendous breakthrough may occur in the field of rock mechanics.

2.4. Preparation of a geotechnical physical model for rock mechanics experiments

Rock mechanics physical model testing, also known as geomechanical model testing, is a physical simulation method that considers certain similarity principles, plays a critical role in the stability evaluation and design of engineering rock masses, and provides insight into certain geotechnical and geomechanical problems [97–99]. However, certain downsides exist in fabricating the physical models of intricate geological structures through conventional approach (e.g., time consuming and low target accuracy), which has become one of the major reasons impeding the development of rock mechanics tests.

Given the advantages of 3DP described previously, 3DP has great potential in the preparation of intricate geotechnical physical models. However, only few investigations have been published in this respect. In 2018, Song *et al.* [15], for the first time, took full advantage of the superiority of 3DP by precisely fabricating several physical tunnel models, including general, single-fault, double-fault, rock bolt, and lining-supported tunnel models which were subjected to a sequence of confined uniaxial compression tests. In accordance with the verified fact in Section 2.1.1, gypsum material exhibits a similar mechanical behavior to real rock, whereas PLA material exhibits obvious ductility and cannot mimic natural rock. Considering such an information, Song *et al.* [15] decided that gypsum and PLA may be adopted to simulate tunnel models and support structures, respectively. They declared that research on physical tunnel models is feasible and applicable via 3DP. This conclusion is ascribed to two issues, namely, i) the failure performance of the general, single-fault tunnel mode is analogous to that of the artificial model and tunnel engineering site, such as an obvious rib spalling phenomenon in the left and right sidewalls, or collapse body formation in the footwall of a fault, and ii) an increase in the loading capacity of the tunnel model due to the support structure (rock bolt and lining), contrary to the results with a fault.

A bearing plate of long-expansion rock bolt was created using 3DP based on a multi-functional powder material, polyamide 12; some laboratory tests were performed on it [100]. Unfortunately, from the results of this previous study, the 3D-printed bearing plate is considered to be invalidated, owing to its lower strength and stiffness than those of the steel bearing plate. Encouragingly, the 3D-printed bearing plate has an appreciable chemoresistance and low weight. According to such previous findings, the development and exploitation of 3DP materials (e.g., improvements in strength and stiffness) can provide a considerable promising means to solve the corrosion of rock bolt bearing plates in actual en-

gineering cases. Moreover, an exploration about essential technologies for manufacturing complex geomechanical physical models using 3DP with rock-like geological materials (e.g., cement and silica sand) is currently being conducted [12]. Tangible geotechnical physical models, which cannot be produced in such ongoing research, may provide an open and novel idea for the fabrication of geotechnical physical models through 3DP with various available materials, particularly geological materials.

2.5. Bridge between the laboratory test and numerical simulation of rock mechanics

As previously noted, the transformation from digital rock model to physical rock specimen was fulfilled via 3DP. Subsequently, the 3D-printed rock specimens allowed us to perform repeated experiments. Simultaneously, in recent studies, digital rock models that experience certain processes, such as 3D reconstruction, mesh generation, or image processing, were also integrated into some frequently-used commercial software (e.g., finite element software, such as rock failure process analysis (RFPA) [50], ANSYS [49,96], and ABAQUS [52]) and discrete element software (e.g., PFC [32], 3DEC [15], and DLSM [20,48]) to conduct a battery of investigations numerically. That is, 3DP complements and counterbalances the gap between experimental testing and numerical simulation, and it may be regarded as a "virtual bridge" linking laboratory experiments and numerical simulations, or as a means of mutual validation between them. In another recent study, 3DP served as a way to verify the reliability of theoretical methods [101].

In 2018, Zhu *et al.* [33], through CT and 3D reconstruction methods, obtained a virtual digital rock model that exhibits the same internal microstructure characteristics as real volcanic rock. To gain insight into the mechanical characteristics and fracture mechanisms of volcanic rock, a digital rock model was transformed via 3DP with transparent resin material, and the resulting physical models were then subjected to a few static and dynamic experimental tests. In addition, the digital rock model was imported into RFPA software to repeatedly conduct corresponding static numerical tests that consider real rock microstructure, which can better reflect rock heterogeneity than a traditional simulation, such as that used in the research of Huang *et al.* [102]. The images presented in Fig. 7 show these three models—natural rock, numerical rock, and 3D-printed rock models—subjected to static Brazilian disc testing. The findings revealed that the path of crack propagation and failure mode in the rock relies on the pre-existing defects at which crack initiation occurs, and the experimental results are in good agreement with the numerical results. These results suggested that the application of 3DP in this field enriches the means of experimental verification and improves the credibility of the test results.

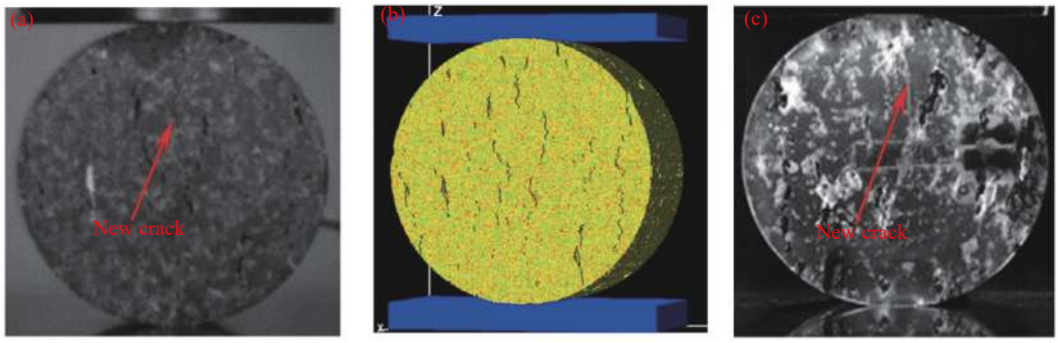

Fig. 7. Schematic of three rock models under static Brazilian disc tests: (a) natural volcanic rock; (b) numerical rock model; (c) 3D-printed rock. Reprinted from *Int. J. Rock Mech. Min. Sci.*, 106, J.B. Zhu, T. Zhou, Z.Y. Liao, L. Sun, X.B. Li, and R. Chen, Replication of internal defects and investigation of mechanical and fracture behaviour of rock using 3D printing and 3D numerical methods in combination with X-ray computerized tomography, 198, Copyright 2018, with permission from Elsevier.

As mentioned in Section 2.3, Ju *et al.* [9,25,32,95] managed to reconstruct and visualize the discontinuous structure inside a natural rock by using a transparent printing material. Moreover, the stress distribution and evolution characteristics around this discontinuous structure were visually reproduced experimentally, with the aid of photoelastic and frozen-stress techniques, under uniaxial compression loads. The corresponding numerical simulation was based on ANSYS and PFC and was performed on an equivalent numerical model with an intricate structure identical to that of the 3D-printed model. The experimental and numerical results exhibited favorable consistency manifested in the fact that high stress concentration areas and stress gradients likely occurred near the discontinuous structure, suggesting that such a structure played a leading role in controlling the mechanical and stress characteristics of the rock. In another study, a 3D-printed pore structure identical to natural rock was applied in an oil–water displacement test to successfully validate the reliability of the lattice Boltzmann simulation [84]. These results once again confirmed that laboratory tests and numerical simulations can be linked via 3DP, and this linkage may greatly improve the credibility of the results to an extent.

3. Discussion

3.1. Improvements in the similarities between 3D-printed and natural rock specimens

In this paper, a systematic comparison made in Section 2.1.1 on the mechanical behaviors (e.g., stress–strain curve, mechanical parameters, failure pattern, and brittleness) between 3D-printed specimens made with different printing materials and real rock suggests that 3D-printed specimens exhibit lower brittleness, lower strength, higher ductility, and lower elastic modulus (higher deformation) than those of real rock under the same situation. The mechanical characteristics of 3D-printed specimens may be artificially modified to become further similar to those of natural rock via some printing configurations and improvement measures [12,103]. The choice of improvement measures, such as freezing, heating, curing, and infiltration, have great reliance on the materials used for 3DP; for instance, ceramic-based 3D-printed specimens are unsuitable for heating treatment after being printed because unexpected cracks appear during heating [27]. Therefore, 3D-printed materials are referred to as the main line to discuss the improvements in the similarities of mechanical behaviors between 3D-printed and natural rock specimens.

The printing orientation and heat treatment of one example were adopted to determine the characteristics of Vero-Clear polymer-based 3DP specimens [104]. Their results suggested that 3D-printed specimens with horizontal layers (inclination angle of 90°) exhibit high strength, including UCS and triaxial compressive strength, and the temperature varies from 120 to 150°C, which can significantly enhance the UCS and direct tensile strength of 3D-printed specimens. However, neither of these methods can increase brittleness. That is, these 3D-printed specimens still showed polymer ductility. Similarly, in other examples, the brittleness of PLA-based 3D-printed specimens can be increased, but the strength is sacrificed by changing their input structure (lattice structure) [10]. Moreover, Vero-Clear and PLA are two typical polymeric materials that exhibit significant ductile behavior. The above description suggests that for polymer-based 3D-printed specimens, the lattice structure model allows such specimens to be heated, which may realize 3D-printed specimens with high strength and favorable brittleness.

Transparent resin material has been proven to be suitable for simulating natural brittle rocks, but brittleness and strength still need further improvements [27]. Fortunately, resin-based 3D-printed specimens treated with dry ice freezing to −77°C, with embedded macrocracks [21], or added micro-defects [33] identical to those of real rock (as determined via micro-CT) exhibited better brittleness than fresh 3D-printed specimens; in addition, the UCS of the frozen 3D-printed resin specimens increased by 73.9% from 110.3 to 191.8 MPa, which was comparable to granite [105]. A splitting failure was observed with strip fragments. Moreover, the stress–strain curve of a frozen 3D-printed resin specimen can be divided into four phases, namely, early nonlinear deformation (concave), elastic deformation, plastic deformation, and post-peak failure, similar to that of natural rock [106], which once again confirmed the feasibility and effectiveness of improving the mechanical behavior of resin-based 3D-printed rock by freezing.

The sand-based 3D-printed specimens made by powder-ink binders are considered to be optimal to simulate weak sandstones [43]. This idea has made researchers consider other factors to improve the similarities in mechanical properties between sand-based 3D-printed and natural sandstone specimens. In one study, raw silica sand was functionalized by silane coupling agents to create a 3D-printed rock with furfuryl alcohol as the binder; the study revealed that the UCS of the functionalized sand-based 3D-printed rock was significantly improved [107], but no obvious brittleness enhancement was observed, as shown in Fig. 8(a). Correspondingly, its mesoscale fracture mechanism determined from scanning electron microscope (SEM) and displayed in Fig. 8(b) exhibited a binder shear failure between sand particles that is universal in real rock. However, this condition was not observed in the 3D-printed rock without functionalization (Fig. 8(c)). These results indicate that the pretreatment of printed material may provide a potential and promising means of guidance for the preparation of optimal sandstone 3DP in the future. In addition to material pretreatment, the influence of printing parameters, such as binder volume fraction (which is equal to the porosity of the specimen multiplied by the binder saturation), on the mechanical behavior of sand-based 3D-printed rock was investigated [29], indicating that binder volume fraction is positively correlated with the UCS of the 3D-printed sandstone, but the volume fraction has a critical value, that is, it cannot exceed 8%; otherwise, a dimensional instability can arise, which means that the increase in the UCS of the 3D-printed sandstone is limited by the varieties of binder content. The posttreatment with respect to curing the sand-based 3D-printed specimens was explored in one investigation [38]. This research declared that the optimum curing temperature for maximizing the mechanical characteristics of the 3D-printed specimen is 80°C, which can avoid the ring hydrolysis of the monomers over the furfuryl alcohol binder. Overall, although none of the above factors are sufficient for sand-based 3D-printed specimens with high strength and favorable brittleness, they can lay a good foundation for seeking a means to reach these properties in future studies.

The size effect of rock is one of the research focuses in the rock mechanics field [108]. In recent studies, this effect was also observed in two gypsum-based 3D-printed cylindrical rock specimens with a height-to-diameter ratio of 2.4 [28,35].

Such research reported that the elasticity modulus of small specimens (25 mm diameter) is approximately twice that of large specimens (50 mm diameter), showing a negative correlation similar to real rock [109]. To an extent, the properties of large 3D-printed specimens were proven to be representatives of real rock, attributing to the fact that they exhibited a more realistic brittleness than small specimens. However, the brittleness and strength were far from those of real rock. To this end, another study examined four factors, namely, layer orientation, layer thickness, binder saturation, and heating treatment, and discussed their impact on the mechanical properties of gypsum-based 3D-printed rocks [16]. We can draw conclusions from their study that printing direction shows an obvious effect on UCS and that printed specimens with vertical layers (inclination angle of 0°) show a maximum UCS, the opposite conclusion previously drawn from polymer-based 3D-printed specimens, suggesting that the anisotropy of 3D-printed specimens is related to printed materials. UCS generally increases as binder saturation increases, and the effect of layer thickness on UCS is not obvious, but a thin layer appears to be advantageous for improving strength and brittleness properties. The optimum temperatures for the good brittleness and maximum UCS of 3D-printed specimens are 70 and 150°C, respectively. This inconsistency means that the heating of gypsum-based 3D-printed specimens is not helpful for achieving high brittleness and strength, and the critical temperature that can counterpoise these two performance metrics is a point for further research. Obviously, the strength of 3D-printed specimens, such as gypsum or polymer specimens, seems to be more sensitive to heating than brittleness. Freezing may currently be one of the most effective ways to make 3D-printed rocks with favorable brittleness and high strength.

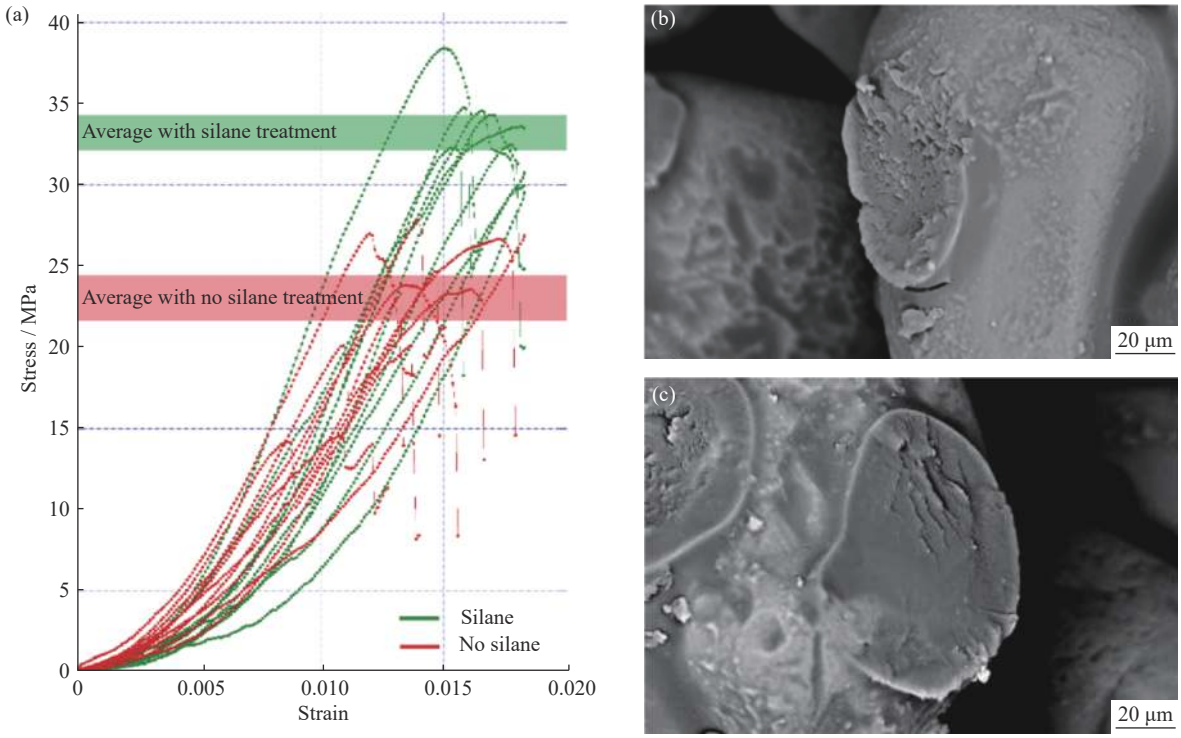

Fig. 8. Comparison of (a) stress–strain curve and binder neck SEM morphology after the uniaxial compression of 3D-printed rock (b) with and (c) without silane treatment. Reprinted from *Int. J. Adhes. Adhes.*, 85, K.J. Hodder, J.A. Nychka, and R.J. Chalaturnyk, Improvement of the unconfined compressive strength of 3D-printed model rock via silica sand functionalization using silane coupling agents, 274, Copyright 2018, with permission from Elsevier.

In our recent research, a series of Brazilian splitting tests on gypsum-based 3D-printed rocks is conducted to investigate the effect of printing orientation on their tensile properties (Fig. 9). As seen from Fig. 9(a), as the printing angle increases, the brittleness characteristics of 3D-printed specimens reduce first, and then increase; as the printing angle is equal to 45°, the specimens show ductility. From Fig. 9(b), as the printing angle increases (from 0° to 90°), the tensile strength and tensile strain exhibit a "V" shape variation trend, that is, they decrease first, and then increase. When the printing angle is equal to 45°, tensile strength and tensile strain reach the lowest values, which are 0.63 MPa and 0.58×10^{-2}, respectively. These results further demonstrate that the printing direction has an obvious effect on the tensile mechanical properties and brittleness characteristics of 3D-printed specimens.

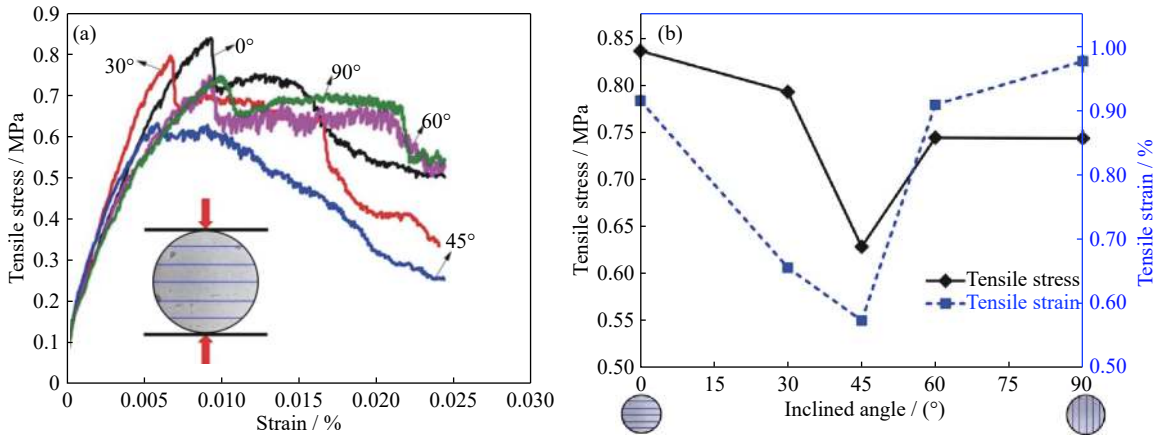

Fig. 9. Effect of printing orientation on the tensile properties of gypsum-based 3D-printed specimens: (a) tensile stress–strain curves; (b) relationship among tensile strength, tensile strain, and printing angle.

3.2. Limitations and prospects of 3DP technology in the application of rock mechanics

Although current 3DP technologies have many unique and clear advantages, certain limitations still remain in rock mechanics application, mainly including the following three aspects:

(1) Limitations of printed materials.

When 3DP technologies are used to prepare rock mechanics specimens, most available 3D-printed rock analogues, such as PLA, Vero-Clear, resin, gypsum, sand, and ceramic rock analogues, generally exhibit high ductility (low brittleness), low strength, and low stiffness (low Young's modulus), all of which are different from the characteristics of natural rock [10,15,32]. Therefore, future research must develop a few novel 3DP materials that can be used alone or together and that exhibit high strength and stiffness, favorable brittleness, and frictional function for preparing 3DP rock analogues that can well stimulate and reproduce the mechanical properties of natural rock.

(2) Limitations of printing accuracy.

When 3DP technologies are utilized to prepare natural or artificial joints to reconstruct rock internal structure and to establish a virtual bridge for experimental testing and numerical simulation, 3D printers with high accuracy are fairly important for research to obtain accurate rock models that lead to reliable and precise research results. However, due to the current limitations of 3D printer resolution, reproducing the internal complex structure of natural rock at the original scale is difficult, requiring specimens to be rescaled to the digital model dimension for the creation of magnified 3D-printed models with partial rock internal structure [85]. Similarly, having a complete materialization on virtual numerical models can be difficult by using current 3D printers, considering that some microscopic pores and cracks play essential roles in numerical models. Therefore, the accuracy of 3D printers should be further improved in the future to address this problem, and doing so can greatly promote the wide application of 3DP technology in rock mechanics. Moreover, if materials similar to natural rock exist and 3D printer accuracy is improved in the future, then directly preparing specimens with natural joints to perform direct shear tests is possible, instead of using current 3D-printed molds with natural joint morphology to cast into direct shear specimens.

(3) Limitations of the printing function.

Currently, most existing 3D printers have only one or two printing nozzles, suggesting that they can only print one or two materials at the same time. Nevertheless, natural rock is a heterogeneous geological body comprising various minerals. Consequently, 3D-printed rock analogues with a single printed material cannot almost reflect the heterogeneity of natural rock [16,33,110]. Thus, future studies should develop printers with multiple nozzles, so that multiple materials can be printed simultaneously. In addition, although 3DP technology can be applied to prepare large geotechnical physical models (compared with standard rock specimens), the sizes of 3D-printed physical models are far from enough compared with actual large-scale physical models in rock mechanics. With the development of 3DP technology, the future 3DP technology should break through the model size and move toward the production of large-sized physical models, which can also promote the development of other fields, including the field of rock mechanics.

4. Conclusions

This review illustrates the development and the state of the art in the application of 3DP technology in the field of rock mechanics. Certain major conclusions in this section are drawn.

(1) A series of rock mechanics tests, including uniaxial and triaxial compression tests, Brazilian disk tests, and SHPB tests, is conducted on 3D-printed rock analogues and natural

rocks (as a control group) to investigate the mechanical properties of 3D-printed rock. The results indicate that the mechanical behaviors, such as stress–strain curve, failure mode, and crack evolution mechanism, of 3D-printed rock shows a similarity with natural rock; however, most 3D-printed rock analogues generally exhibit high ductility, low strength, and low stiffness. Specifically, low stiffness, which means large strain, can be observed in the 3D-printed rock analogues of all material types, and nearly no 3D-printed rock analogues with high strength, favorable brittleness, and large stiffness are found in the published investigations. Although few improvement measures, such as optimization of printing parameters (binder saturation, printing layer thickness, and orientation) and postprocessing (freezing or heating), may be currently adopted in controlling the mechanical behaviors of these 3D-printed analogues, such measures cannot be achieved with either of the previous properties.

(2) Rock-like specimens, with pre-existing flaws, fabricated by 3DP exhibit exceedingly perfect dominant positions, such as simple flaw prefabrication, geometric flexibility, rapid prototyping, and material homogeneity, over conventional means. Moreover, the dynamic crack evolution process observed in 3D-printed flawed specimens is comparable to those in natural rocks, concrete specimens, and numerical models, indicating the feasibility of 3DP in the investigation of rock-like materials undergoing deformation and progressive failure.

(3) Verifying tests, including geometrical verification among original joints (virgin or Barton's joints), 3D-printed joint molds, and testing joint specimens and shearing testing verification on testing joint specimens, suggest that 3DP (coupled with 3D scanning) enables us to perfectly replicate natural and artificial joints with fairly good accuracy. Moreover, testing joint specimens based on 3D-printed molds under analogous testing conditions exhibit uniform shearing properties, such as shearing strength (or deformation curve) and shearing failure location.

(4) 3DP, coupled with other advanced technologies (e.g., CT scanning, photoelastic testing, and stress freezing), allows us to reproduce and visualize complex natural rock structures and to elucidate inherent physical and mechanical processes and microscopic mechanisms inside rock masses, thereby providing new research opportunities regarding deep rock mechanics. However, mechanical similarities between 3D-printed reconstruction models and their corresponding prototypes require further improvement.

(5) A preliminary investigation on the preparation of a geotechnical physical model adopting 3DP technology suggests that 3DP exhibits feasibility and applicability in this aspect to an extent. Regrettably, the printing size of the 3D-printed geophysical model has certain limitations due to current technical conditions.

Acknowledgements

This work was financially supported by the Fundamental Research Funds for the Central Universities (No. FRF-TP-18-016A3) and the National Natural Science Foundation of China (No. 51504016).

References

[1] B.H.G. Brady and E.T. Brown, *Rock Mechanics: For Underground Mining*, George Allen & Unwin Ltd, London, 1985, p. 15.

[2] R.E. Goodman, *Introduction to Rock Mechanics*, 2nd ed., Wiley, New York, 1989, p. 28.

[3] R.D. Lama and V.S. Vutukuri, *Handbook on Mechanical Properties of Rocks*, Trans Tech Publications, Clausthal, 1978, p. 116.

[4] W.R. Wawersik and C. Fairhurst, A study of brittle rock fracture in laboratory compression experiments, *Int. J. Rock Mech. Min. Sci.*, 7(1970), No. 5, p. 561.

[5] Y. Zhou, G. Zhang, S.C. Wu, and L. Zhang, The effect of flaw on rock mechanical properties under the Brazilian test, *Kuwait J. Sci.*, 45(2018), No. 2, p. 94.

[6] S.W. Feng, Y. Zhou, Y. Wang, and M.D. Lei, Experimental research on the dynamic mechanical properties and damage characteristics of lightweight foamed concrete under impact loading, *Int. J. Impact Eng.*, 140(2020), art. No. 103558.

[7] Y. Zhou, S.C. Wu, Y.T. Gao, and A. Misra, Macro and meso analysis of jointed rock mass triaxial compression test by using equivalent rock mass (ERM) technique, *J. Cent. South Univ.*, 21(2014), No. 3, p. 1125.

[8] Y. Zhou, N.B. Chen, L. Wang, J.W. Li, and T.H. Wu, A flat-joint contact model and meso analysis on mechanical characteristics of brittle rock, *Kuwait J. Sci.*, 46(2019), No. 3, p. 71.

[9] Y. Ju, H.P. Xie, Z.M. Zheng, J.B. Lu, L.T. Mao, F. Gao, and R.D. Peng, Visualization of the complex structure and stress field inside rock by means of 3D printing technology, *Chin. Sci. Bull.*, 59(2014), No. 36, p. 5354.

[10] C. Jiang and G.F. Zhao, A preliminary study of 3D printing on rock mechanics, *Rock Mech. Rock Eng.*, 48(2015), No. 3, p. 1041.

[11] M. Sharafisafa, L.M. Shen, and Q.F. Xu, Characterisation of mechanical behaviour of 3D printed rock-like material with digital image correlation, *Int. J. Rock Mech. Min. Sci.*, 112(2018), p. 122.

[12] X.T. Feng, Y.H. Gong, Y.Y. Zhou, Z.W. Li, and X.F. Liu, The 3D-printing technology of geological models using rock-like materials, *Rock Mech. Rock Eng.*, 52(2019), p. 2261.

[13] C.W. Hull, *Apparatus for Production of Three-Dimensional Objects by Stereolithography*, United States Patent, Appl. 4575330, 1986.

[14] S. Bose, S. Vahabzadeh, and A. Bandyopadhyay, Bone tissue engineering using 3D printing, *Mater. Today*, 16(2013), No. 12, p. 496.

[15] L.B. Song, Q. Jiang, Y.E. Shi, X.T. Feng, Y.H. Li, F.S. Su, and C. Liu, Feasibility investigation of 3D printing technology for geotechnical physical models: Study of tunnels, *Rock Mech. Rock Eng.*, 51(2018), p. 2617.

[16] S. Fereshtenejad and J.J. Song, Fundamental study on applicability of powder-based 3D printer for physical modeling in

rock mechanics, *Rock Mech. Rock Eng.*, 49(2016), No. 6, p. 2065.

[17] P. Liu, Y. Ju, P.G. Ranjith, Z.M. Zheng, L. Wang, and A. Wanniarachchi, Visual representation and characterization of three-dimensional hydrofracturing cracks within heterogeneous rock through 3D printing and transparent models, *Int. J. Coal Sci. Technol.*, 3(2016), No. 3, p. 284.

[18] H. Mazhar, T. Osswald, and D. Negrut, On the use of computational multi-body dynamics analysis in SLS-based 3D printing, *Addit. Manuf.*, 12(2016), p. 291.

[19] M.G. Mitchell, *Cell Biology: Translational Impact in Cancer Biology and Bioinformatics*, Elsevier, Cambridge, 2016, p. 122.

[20] C. Jiang, G.F. Zhao, J.B. Zhu, Y.X. Zhao, and L.M. Shen, Investigation of dynamic crack coalescence using a gypsum-like 3D printing material, *Rock Mech. Rock Eng.*, 49(2016), No. 10, p. 3983.

[21] T. Zhou, J.B. Zhu, Y. Ju, and H.P. Xie, Volumetric fracturing behavior of 3D printed artificial rocks containing single and double 3D internal flaws under static uniaxial compression, *Eng. Fract. Mech.*, 205(2019), p. 190.

[22] E.M. Gell, S.M. Walley, and C.H. Braithwaite, Review of the validity of the use of artificial specimens for characterizing the mechanical properties of rocks, *Rock Mech. Rock Eng.*, 52(2019), No. 9, p. 2949.

[23] R.M. Bishwal, Scope of 3-D printing in mining and geology: An overview, *J. Geol. Soc. India*, 93(2019), No. 4, p. 482.

[24] Q. Jiang, X.T. Feng, L.B. Song, Y.H. Gong, H. Zheng, and J. Cui, Modeling rock specimens through 3D printing: Tentative experiments and prospects, *Acta Mech. Sin.*, 32(2016), No. 1, p. 101.

[25] Y. Ju, L. Wang, H.P. Xie, G.W. Ma, L.T. Mao, Z.M. Zheng, and J.B. Lu, Visualization of the three-dimensional structure and stress field of aggregated concrete materials through 3D printing and frozen-stress techniques, *Constr. Build. Mater.*, 143(2017), p. 121.

[26] T. Zhou and J.B. Zhu, An experimental investigation of tensile fracturing behavior of natural and artificial rocks in static and dynamic Brazilian disc tests, *Procedia Eng.*, 191(2017), p. 992.

[27] T. Zhou and J.B. Zhu, Identification of a suitable 3D printing material for mimicking brittle and hard rocks and its brittleness enhancements, *Rock Mech. Rock Eng.*, 51(2018), No. 3, p. 765.

[28] L.Y. Kong, M. Ostadhassan, C.X. Li, and N. Tamimi, Can 3-D printed gypsum samples replicate natural rocks? An experimental study, *Rock Mech. Rock Eng.*, 51(2018), No. 10, p. 3061.

[29] K.J. Hodder, J.A. Nychka, and R.J. Chalaturnyk, Process limitations of 3D printing model rock, *Prog. Addit. Manuf.*, 3(2018), p. 173.

[30] X. Wang, M. Jiang, Z.W. Zhou, J.H. Gou, and D. Hui, 3D printing of polymer matrix composites: A review and prospective, *Composites Part B*, 110(2017), p. 442.

[31] T.D. Ngo, A. Kashani, G. Imbalzano, K.T.Q. Nguyen, and D. Hui, Additive manufacturing (3D printing): A review of materials. methods.applications and challenges, *Composites Part B*, 143(2018), p. 172.

[32] Y. Ju, L. Wang, H.P. Xie, G.W. Ma, Z.M. Zheng, and L.T. Mao, Visualization and transparentization of the structure and stress field of aggregated geomaterials through 3D printing and photoelastic techniques, *Rock Mech. Rock Eng.*, 50(2017), No. 6, p. 1383.

[33] J.B. Zhu, T. Zhou, Z.Y. Liao, L. Sun, X.B. Li, and R. Chen, Replication of internal defects and investigation of mechanical and fracture behaviour of rock using 3D printing and 3D numerical methods in combination with X-ray computerized tomography, *Int. J. Rock Mech. Min. Sci.*, 106(2018), p. 198.

[34] T. Zhou and J.B. Zhu, Application of 3D printing and micro-CT scan to rock dynamics, [in] H.B. Li, J.C. Li, Q.B. Zhang, and J. Zhao, eds., *Rock Dynamics: From Research to Engineering, 2nd International Conference on Rock Dynamics and Applications*, Suzhou, 2016, p. 247.

[35] L.Y. Kong, M. Ostadhassan, C.X. Li, and N. Tamimi, Rock physics and geomechanics of 3-D printed rocks, [in] *51st U.S. Rock Mechanics/Geomechanics Symposium*, San Francisco, 2017, p. 2866.

[36] S.Q. Yang, P.F. Yin, and P.G. Ranjith, Experimental study on mechanical behavior and brittleness characteristics of Longmaxi formation shale in Changning, Sichuan basin, China, *Rock Mech. Rock Eng.*, 53(2020), p. 2461.

[37] S. Osinga, G. Zambrano-Narvaez, and R.J. Chalaturnyk, Study of geomechanical properties of 3D printed sandstone analogue, [in] *49th US Rock Mechanics/Geomechanics Symposium*, San Francisco, 2015, p. 3137.

[38] B. Primkulov, J. Chalaturnyk, R. Chalaturnyk, and G. Zambrano-Narvaez, 3D printed sandstone strength: Curing of furfuryl alcohol resin-based sandstones, *3D Print. Addit. Manuf.*, 4(2017), No. 3, p. 149.

[39] D. Vogler, S.D.C. Walsh, E. Dombrovski, and M.A. Perras, A comparison of tensile failure in 3D-printed and natural sandstone, *Eng. Geol.*, 226(2017), p. 221.

[40] M.A. Perras and D. Vogler, Compressive and tensile behavior of 3D-printed and natural sandstones, *Transp. Porous Media*, 129(2019), No. 2, p. 559.

[41] J.S. Gomez, R.J. Chalaturnyk, and G. Zambrano-Narvaez, Experimental investigation of the mechanical behavior and permeability of 3D printed sandstone analogues under triaxial conditions, *Transp. Porous Media*, 129(2019), No. 2, p. 541.

[42] W. Tian and N.V. Han, Mechanical properties of rock specimens containing pre-existing flaws with 3D printed materials, *Strain*, 53(2017), No. 6, art. No. e12240.

[43] W. Tian and N.V. Han, Preliminary research on mechanical properties of 3D printed rock structures, *Geotech. Test. J.*, 40(2017), No. 3, p. 483.

[44] S.Q. Yang, Crack coalescence behavior of brittle sandstone samples containing two coplanar fissures in the process of deformation failure, *Eng. Fract. Mech.*, 78(2011), No. 17, p. 3059.

[45] T.H. Wu, Y.T. Gao, Y. Zhou, and J.W. Li, Experimental and numerical study on the interaction between holes and fissures in rock-like materials under uniaxial compression, *Theor. Appl. Fract. Mech.*, 106(2020), art. No. 102488.

[46] J.X. Zhou, Y. Zhou, and Y.T. Gao, Effect mechanism of fractures on the mechanics characteristics of jointed rock mass under compression, *Arab. J. Sci. Eng.*, 43(2018), No. 7, p. 3659.

[47] J. Hiller and H. Lipson, Design and analysis of digital materials for physical 3D voxel printing, *Rapid PrototyJ.*, 15(2009), No. 2, p. 137.

[48] C. Jiang and G.F. Zhao, Implementation of a coupled plastic damage distinct lattice spring model for dynamic crack propagation in geomaterials, *Int. J. Numer. Anal. Methods Geomech.*, 42(2018), No. 4, p. 674.

[49] Y. Ju, Z. Zheng, H. Xie, J. Lu, L. Wang, and K. He, Experimental visualisation methods for three-dimensional stress fields of porous solids, *Exp. Tech.*, 41(2017), No. 4, p. 331.

[50] G.W. Ma, Q.Q. Dong, L.F. Fan, and J.W. Gao, An investigation of non-straight fissures cracking under uniaxial compression, *Eng. Fract. Mech.*, 191(2018), p. 300.
[51] Y. Ju, H.P. Xie, X. Zhao, L.T. Mao, Z.Y. Ren, J.T. Zheng, F.P. Chiang, Y.L. Wang, and F. Gao, Visualization method for stress-field evolution during rapid crack propagation using 3D printing and photoelastic testing techniques, *Sci. Rep.*, 8(2018), No. 1, art. No. 4353.
[52] G.W. Ma, Q.Q. Dong, and L. Wang, Experimental investigation on the cracking behavior of 3D printed kinked fissure, *Sci. China Technol. Sci.*, 61(2018), No. 12, p. 1872.
[53] H. Haeri, K. Shahriar, M.F. Marji, and P. Moarefvand, Experimental and numerical study of crack propagation and coalescence in pre-cracked rock-like disks, *Int. J. Rock Mech. Min. Sci.*, 67(2014), p. 20.
[54] H. Haeri, A. Khaloo, and M.F. Marji, Experimental and numerical analysis of Brazilian discs with multiple parallel cracks, *Arabian J. Geosci.*, 8(2015), No. 8, p. 5897.
[55] M. Sharafisafa, L.M. Shen, Y.G. Zheng, and J.Z. Xiao, The effect of flaw filling material on the compressive behaviour of 3D printed rock-like discs, *Int. J. Rock Mech. Min. Sci.*, 117(2019), p. 105.
[56] R.E. Goodman, R.L. Taylor, and T.L. Brekke, A model for the mechanics of jointed rock, *J. Soil Mech. Found. Div*, 94(1968), No. 3, p. 637.
[57] S. Bandis, A.C. Lumsden, and N.R. Barton, Experimental studies of scales effects on the shear behaviour of rock joints, *Int. J. Rock Mech. Min. Sci.*, 18(1981), No. 1, p. 1.
[58] J.W. Park and J.J. Song, Numerical simulation of a direct shear test on a rock joint using a bonded-particle model, *Int. J. Rock Mech. Min. Sci.*, 46(2009), No. 8, p. 1315.
[59] Z.T. Bieniawski, Determining rock mass deformability: Experience from case histories, *Int. J. Rock Mech. Min. Sci.*, 15(1978), No. 5, p. 237.
[60] T.S. Ueng, Y.J. Jou, and I.H. Peng, Scale effect on shear strength of computer-aided-manufactured joints, *J. GeoEng.*, 5(2010), No. 2, p. 29.
[61] R. Kumar and A.K. Verma, Anisotropic shear behavior of rock joint replicas, *Int. J. Rock Mech. Min. Sci.*, 90(2016), p. 62.
[62] Y. Gui, C.C. Xia, W.Q. Ding, X. Qian, and S.G. Du, A new method for 3D modeling of joint surface degradation and void space evolution under normal and shear loads, *Rock Mech. Rock Eng.*, 50(2017), p. 2827.
[63] Y. Fang, D. Elsworth, T. Ishibashi, and F.S. Zhang, Permeability evolution and frictional stability of fabricated fractures with specified roughness, *J. Geophys. Res. Solid Earth*, 123(2018), No. 11, p. 9355.
[64] M. Asadizadeh, M. Moosavi, M.F. Hossaini, and H. Masoumi, Shear strength and cracking process of non-persistent jointed rocks: An extensive experimental investigation, *Rock Mech. Rock Eng.*, 51(2018), No. 2, p. 415.
[65] M. Asadizadeh, M.F. Hossaini, M. Moosavi, H. Masoumi, and P.G. Ranjith, Mechanical characterisation of jointed rock-like material with non-persistent rough joints subjected to uniaxial compression, *Eng. Geol.*, 260(2019), art. No. 105224.
[66] Y.J. Xia, C.Q. Zhang, H. Zhou, J. Hou, G.S. Su, Y. Gao, N. Liu, and H.K. Singh, Mechanical behavior of structurally reconstructed irregular columnar jointed rock mass using 3D printing, *Eng. Geol.*, 268(2020), art. No. 105509.
[67] N. Barton and V. Choubey, The shear strength of rock joints in theory and practice, *Rock Mech.*, 10(1977), p. 1.
[68] D.H. Kim, I. Gratchev, M. Hein, and A. Balasubramaniam, The application of normal stress reduction function in tilt tests for different block shapes, *Rock Mech. Rock Eng.*, 49(2016), No. 8, p. 3041.
[69] Q.S. Liu, Y.C. Tian, P.Q. Ji, and H. Ma, Experimental investigation of the peak shear strength criterion based on three-dimensional surface description, *Rock Mech. Rock Eng.*, 51(2018), p. 1005.
[70] L.B. Gong, A. Heitor, and B. Indraratna, An approach to measure infill matric suction of irregular infilled rock joints under constant normal stiffness shearing, *J. Rock Mech. Geotech. Eng.*, 10(2018), No. 4, p. 653.
[71] Y.B. Huang, Y.J. Zhang, Z.W. Yu, Y.Q. Ma, and C. Zhang, Experimental investigation of seepage and heat transfer in rough fractures for enhanced geothermal systems, *Renewable Energy*, 135(2019), p. 846.
[72] S. Choi, S. Lee, H. Jeong, and S. Jeon, Development of a new method for the quantitative generation of an artificial joint specimen with specific geometric properties, *Sustainability*, 11(2019), No. 2, art. No. 373.
[73] B. Indraratna, A. Haque, and N. Aziz, Laboratory modelling of shear behaviour of soft joints under constant normal stiffness conditions, *Geotech. Geol. Eng.*, 16(1998), p. 17.
[74] J. Woodman, W. Murphy, M.E. Thomas, A. Ougier-Simonin, H. Reeves, and T.W. Berry, A novel approach to the laboratory testing of replica discontinuities: 3D printing representative morphologies, [in] *51st US Rock Mechanics/Geomechanics Symposium*. San Francisco, 2017, p. 143.
[75] Y.J. Xia, C.Q. Zhang, H. Zhou, J.L. Chen, Y. Gao, N. Liu, and P.Z. Chen, Structural characteristics of columnar jointed basalt in drainage tunnel of Baihetan hydropower station and its influence on the behavior of P-wave anisotropy, *Eng. Geol.*, 264(2020), art. No. 105304.
[76] Q. Jiang, X.T. Feng, Y.H. Gong, L.B. Song, S.G. Ran, and J. Cui, Reverse modelling of natural rock joints using 3D scanning and 3D printing, *Comput. Geotech.*, 73(2016), p. 210.
[77] M.R. Shen and Q.Z. Zhang, Experimental study of shear deformation characteristics of rock mass discontinuities, *Chin. J. Rock Mech. Eng.*, 29(2010), No. 4, p. 713.
[78] Z.X. Zou, H.M. Tang, X. Liu, R. Yong, and W.D. Ni, Quantitative study of structural plane direct shear test results influenced by sample preparation errors, *Chin. J. Rock Mech. Eng.*, 29(2010), No. 8, p. 1664.
[79] J.C. Li, L.F. Rong, H.B. Li, and S.N. Hong, An SHPB test study on stress wave energy attenuation in jointed rock masses, *Rock Mech. Rock Eng.*, 52(2019), p. 403.
[80] Y. Ju, Y.M. Yang, Z.D. Song, and W.J. Xu, A statistical model for porous structure of rocks, *Sci. China Ser. E: Technol. Sci.*, 51(2008), No. 11, p. 2040.
[81] Y. Ju, Q.G. Zhang, Y.M. Yang, H.P. Xie, F. Gao, and H.J. Wang, An experimental investigation on the mechanism of fluid flow through single rough fracture of rock, *Sci. China Technol. Sci.*, 56(2013), No. 8, p. 2070.
[82] A. Suzuki, S. Sawasdee, H. Makita, T. Hashida, K.W. Li, and R.N. Horne, Characterization of 3D printed fracture networks, [in] *Proceedings of the 41st Workshop on Geothermal Reservoir Engineering*, Stanford, 2016.
[83] A. Suzuki, N. Watanabe, K.W. Li, and R.N. Horne, Fracture network created by 3-D printer and its validation using CT images, *Water Resour. Res.*, 53(2017), No. 7, p. 6330.
[84] Y. Ju, W.B. Gong, and J.T. Zheng, Characterization of immiscible phase displacement in heterogeneous pore structures: Parallel multicomponent lattice Boltzmann simulation and experimental validation using three-dimensional printing technology, *Int. J. Multiphase Flow*, 114(2019), p. 50.

[85] S. Ishutov, *3D Printing Porous Proxies as a New Tool for Laboratory and Numerical Analyses of Sedimentary Rocks* [Dissertation], Iowa State University, Ames, 2017, p. 102.

[86] S. Ishutov, F.J. Hasiuk, C. Harding, and J.N. Gray, 3D printing sandstone porosity models, *Interpretation*, 3(2015), No. 3, p. SX49.

[87] S. Ishutov and F.J. Hasiuk, 3D printing Berea sandstone: Testing a new tool for petrophysical analysis of reservoirs, *Petrophysics*, 58(2017), No. 6, p. 592.

[88] S. Ishutov, F.J. Hasiuk, S.M. Fullmer, A.S. Buono, J.N. Gray, and C. Harding, Resurrection of a reservoir sandstone from tomographic data using three-dimensional printing, *AAPG Bull.*, 101(2017), No. 9, p. 1425.

[89] S. Ishutov, F.J. Hasiuk, D. Jobe, and S. Agar, Using resin-based 3D printing to build geometrically accurate proxies of porous sedimentary rocks, *Groundwater*, 56(2018), No. 3, p. 482.

[90] F. Hasiuk, S. Ishutov, and A. Pacyga, Validating 3D-printed porous proxies by tomography and porosimetry, *Rapid Prototyp. J.*, 24(2018), No. 3, p. 630.

[91] S. Ishutov, Establishing framework for 3D printing porous rock models in curable resins, *Transp. Porous Media*, 129(2019), p. 431.

[92] L.Y. Kong, M. Ostadhassan, C.X. Li, and N. Tamimi, Pore characterization of 3D-printed gypsum rocks: A comprehensive approach, *J. Mater. Sci.*, 53(2018), p. 5063.

[93] A. Piovesan, C. Achille, R. Ameloot, B. Nicolai, and P. Verboven, Pore network model for permeability characterization of three-dimensionally-printed porous materials for passive microfluidics, *Phys. Rev. E*, 99(2019), No. 3, art. No. 033107.

[94] D. Head and T. Vanorio, Effects of changes in rock microstructures on permeability: 3-D printing investigation, *Geophys. Res. Lett.*, 43(2016), No. 14, p. 7494.

[95] Y. Ju, Z.Y. Ren, L.T. Mao, and F.P. Chiang, Quantitative visualisation of the continuous whole-field stress evolution in complex pore structures using photoelastic testing and 3D printing methods, *Opt. Express*, 26(2018), No. 5, p. 6182.

[96] Y. Ju, Z.Y. Ren, X.L. Li, Y.T. Wang, L.T. Mao, and F.P. Chiang, Quantification of hidden whole-field stress inside porous geomaterials via three-dimensional printing and photoelastic testing methods, *J. Geophys. Res. Solid Earth*, 124(2019), No. 6, p. 5408.

[97] M.C. He, W.L. Gong, H.M. Zhai, and H.P. Zhang, Physical modeling of deep ground excavation in geologically horizontal strata based on infrared thermography, *Tunnelling Underground Space Technol.*, 25(2010), No. 4, p. 366.

[98] X.T. Feng, S.F. Pei, Q. Jiang, Y.Y. Zhou, S.J. Li, and Z.B. Yao, Deep fracturing of the hard rock surrounding a large underground cavern subjected to high geostress: *In situ* observation and mechanism analysis, *Rock Mech. Rock Eng.*, 50(2017), p. 2155.

[99] Q.Y. Zhang, K. Duan, Y.Y. Jiao, and W. Xiang, Physical model test and numerical simulation for the stability analysis of deep gas storage cavern group located in bedded rock salt formation, *Int. J. Rock Mech. Min. Sci.*, 94(2017), p. 43.

[100] K. Skrzypkowski, W. Korzeniowski, K. Zagórski, and P. Dudek, Application of long expansion rock bolt support in the underground mines of Legnica–Głogów copper district, *Stud. Geotech. Mech.*, 39(2017), No. 3, p. 47.

[101] L.Y. Kong, M. Ostadhassan, S. Zamiran, B. Liu, C.X. Li, and G.G. Marino, Geomechanical upscaling methods: Comparison and verification via 3D printing, *Energies*, 12(2019), No. 3, p. 382.

[102] Y.H. Huang, S.Q. Yang, and W.L. Tian, Cracking process of a granite specimen that contains multiple pre-existing holes under uniaxial compression, *Fatigue Fract. Eng. Mater. Struct.*, 42(2019), No. 6, p. 1341.

[103] A. Farzadi, M. Solati-Hashjin, M. Asadi-Eydivand, and N.A.A. Osman, Effect of layer thickness and printing orientation on mechanical properties and dimensional accuracy of 3D printed porous samples for bone tissue engineering, *PLoS One*, 9(2014), No. 9, art. No. e108252.

[104] L. Wang, Y. Ju, H.P. Xie, G.W. Ma, L.T. Mao, and K.X. He, The mechanical and photoelastic properties of 3D printable stress-visualized materials, *Sci. Rep.*, 7(2017), No. 1, art. No. 10918.

[105] O. Sano, I. Ito, and M. Terada, Influence of strain rate on dilatancy and strength of Oshima granite under uniaxial compression, *J. Geophys. Res. Solid Earth*, 86(1981), No. B10, p. 9299.

[106] C.D. Martin, *The Strength of Massive Lac Du Bonnet Granite Around Underground Openings* [Dissertation], University of Manitoba, Winnipeg, 1993, p. 12.

[107] K.J. Hodder, J.A. Nychka, and R.J. Chalaturnyk, Improvement of the unconfined compressive strength of 3D-printed model rock via silica sand functionalization using silane coupling agents, *Int. J. Adhes. Adhes.*, 85(2018), p. 274.

[108] M. Haftani, B. Bohloli, A. Nouri, M.R.M. Javan, and M. Moosavi, Size effect in strength assessment by indentation testing on rock fragments, *Int. J. Rock Mech. Min. Sci.*, 65(2014), p. 141.

[109] P.T. Wang, T.H. Yang, T. Xu, M.F. Cai, and C.H. Li, Numerical analysis on scale effect of elasticity, strength and failure patterns of jointed rock masses, *Geosci. J.*, 20(2016), No. 4, p. 539.

[110] P. Feng, X.M. Meng, J.F. Chen, and L.P. Ye, Mechanical properties of structures 3D printed with cementitious powders, *Constr. Build. Mater.*, 93(2015), p. 486.